Nanosecond Fluctuations of the Molecular Backbone of Collagen in Hard and Soft Tissues: A Carbon-13 Nuclear Magnetic Resonance Relaxation Study

Susanta K. Sarkar,‡ Catherine E. Sullivan, and Dennis A. Torchia*

Mineralized Tissue Research Branch, National Institute of Dental Research, National Institutes of Health, Bethesda, Maryland 20205

Received July 30, 1984

ABSTRACT: We have determined the amplitude of nanosecond fluctuations of the collagen azimuthal orientation in intact tissues and reconstituted fibers from an analysis of ^{13}C NMR relaxation data. We have labeled (a) intact rat calvaria and tibia collagen (mineralized and cross-linked), (b) intact rat tail tendon and demineralized bone collagen (cross-linked), and (c) reconstituted lathyritic (non-cross-linked) chick calvaria collagen with [2-^{13}C]glycine. This label was chosen because one-third of the amino acid residues in collagen are glycine and because the ^1H–^{13}C dipolar coupling is the dominant relaxation mechanism. Spin–lattice relaxation times (T_1) and nuclear Overhauser enhancements were measured at 15.09 and 62.98 MHz at 22 and −35 °C. The measured NMR parameters have been analyzed by using a dynamic model in which the azimuthal orientation of the molecule fluctuates as a consequence of reorientation about the axis of the triple helix. We have shown that if root mean square fluctuations in the azimuthal orientations are small, $\gamma_{rms} \ll 1$ rad, (a) the correlation function decays with a single correlation time τ and (b) T_1 depends only upon τ and γ_{rms} and not the detailed model of motion. Our analysis shows that, at 22 °C, τ is in the 1–5-ns range for all samples and γ_{rms} is 10°, 9°, and 5.5° for the non-cross-linked, cross-linked, and mineralized samples, respectively. At −35 °C, γ_{rms} is less than 3° for all samples. These results show that mineral and low temperature significantly restrict the amplitude of nanosecond motions of the collagen backbone. Similar conclusions were obtained from an analysis of [1-^{13}C]glycine line shapes, except that the γ_{rms} values reported were 3–4 times larger than γ_{rms} values reported herein. We suggest this difference in γ_{rms} values is obtained because line shapes are sensitive to much slower motions than are relaxation parameters.

We have recently measured ^{13}C nuclear magnetic resonance (NMR)[1] line shapes in order to study the dynamics of the collagen backbone as a function of cross-linking and mineralization in intact tissues (Sarkar et al., 1983). Analysis of [1-^{13}C]glycine line shapes has shown that cross-linking and mineralization restrict reorientation of the collagen backbone. The [1-^{13}C]glycine line shapes studied were sensitive to motions having correlation times $\lesssim 10^{-4}$ s. It was found that, on this time scale, the root mean square fluctuations in the collagen azimuthal angle, γ_{rms}, were 41°, 31°, and 14°, respectively, for un-cross-linked, cross-linked, and mineralized collagen at 22 °C (Sarkar et al., 1983).

Preliminary spin–lattice relaxation, T_1, data on [1-^{13}C]-glycine-labeled collagen suggested that (a) the amplitude of fast (nanosecond) backbone motions was significantly smaller than the amplitude of slow ($\tau \lesssim 10^{-4}$ s) motions and (b) the amplitude of the fast motions was affected by cross-links and mineral. However, a quantitative analysis of the spin–lattice relaxation data was complicated by two problems. First, two relaxation mechanisms (Spiess, 1978), chemical shift anisotropy and proton–carbon dipolar coupling, contributed to spin–lattice relaxation at the field strength (5.9 T) of our experiment. Second, observed T_1 values were so large (8–10 s) that the spin–lattice relaxation may have been affected by ^{13}C–^{13}C spin diffusion (Caravatti et al., 1982; Szeverenyi et al., 1982; Henrichs & Linder, 1984).

We have circumvented these problems by preparing collagen labeled with [2-^{13}C]glycine. The labeled methylene carbon has a small chemical shift anisotropy ($\sigma_{zz} - \sigma_{xx} \leq 50$ ppm) and a large proton–carbon dipolar coupling ($\omega_D/2\pi = 23$ kHz). Therefore, a single mechanism, ^1H–^{13}C dipolar coupling, is responsible for spin–lattice relaxation. Furthermore, the strong dipolar interaction makes the ^{13}C T_1 values at 22 °C much less than the time required for ^{13}C–^{13}C spin diffusion. We have analyzed spin–lattice relaxation times and nuclear Overhauser enhancement (NOE) values measured at two fields, and we report herein the effect of cross-linking, mineralization, and temperature on the amplitude of rapid motions ($\tau \sim 10^{-9}$ s) of the collagen backbone.

Materials and Methods

[2-^{13}C]Glycine (90 atom % ^{13}C) was purchased from Merck Isotopes (Canada). It was characterized by elemental and amino acid analyses and mass spectrometry before use.

Reconstituted collagen fibrils labeled with [2-^{13}C]glycine were prepared by means of chick calvaria tissue culture as described by Jelinski & Torchia (1979). The collagen fibrils, in equilibrium with 0.02 M Na_2HPO_4, were packed into NMR tubes. Intact tissues were labeled by subcutaneous injection of a saline solution of [2-^{13}C]glycine (1.3 M) in the following manner. Beginning with 3-day-old rats 300 μL/day of glycine solution was injected for 5 days. Injection volume was increased to 500 μL for the next 7 days and finally to 700 μL

‡Present address: Laboratory of Chemical Physics, National Institute of Arthritis, Diabetes and Digestive and Kidney Diseases, National Institutes of Health, Bethesda, MD 20205.

[1] Abbreviations: NMR, nuclear magnetic resonance; γ_{rms}, root mean square fluctuation in the collagen azimuthal angle; T_1, spin–lattice relaxation time; NOE, nuclear Overhauser enhancement; τ, rotational correlation time; σ_{xx}, σ_{yy}, and σ_{zz}, the principal values of the chemical shift tensor relative to the isotropic value, σ_i, in the convention (Spiess, 1978) $|\sigma_{zz}| > |\sigma_{xx}| > |\sigma_{yy}|$; ω_D, ^1H–^{13}C dipolar coupling constant as defined by Torchia & Szabo (1982); $\hat{\mu}$, unit vector parallel to the C–H bond axis.

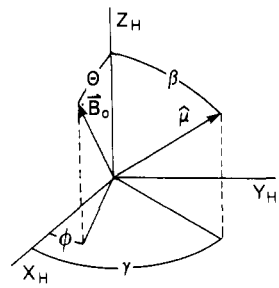

FIGURE 1: Illustration of the (X_H, Y_H, Z_H) coordinate system used to derive relaxation equations. Z_H is parallel to the helix axis, (β, γ) are the polar angles of the unit vector $\hat{\mu}$, where $\hat{\mu}$ is along the C^{α}–H bond, and (θ, ϕ) are the polar angles of B_0.

from day 15 through day 20. The rats were sacrificed on the 21st day, and the calvaria, tail tendons, and tibia were removed. They were washed, defatted, equilibrated with 0.15 M NaCl, and packed into NMR tubes. In each case, control samples were obtained in a similar manner except that unlabeled glycine was used instead of the labeled material.

Amino acid analyses of collagen hydrolysates were obtained by using a Durrum automatic amino acid analyzer. By use of the methods described previously (Sarkar et al., 1983), mineral content in the calvaria and tibia samples was found to be ~55%, indicating essentially complete mineralization (Eanes, 1973).

Gas chromatography/mass spectroscopic analysis of the *N*-acetylmethyl ester derivatives of the protein hydrolysates showed that the level of enrichment was 30% in the rat tissue collagens and 50% in the reconstituted chick collagen fibers.

^{13}C NMR spectra were obtained at 15.09 and 62.98 MHz on home-built solid-state spectrometers (Jelinski & Torchia, 1979; Sarkar et al., 1983). The 90° carbon pulse width was 5–6 μs, and the proton decoupling field [$\gamma_2 B_2/(2\pi)$] was 40–50 kHz. The free induction decay (FID) signals were detected in quadrature by using 1024 and 2048 data points/channel at 15.09 and 62.98 MHz, respectively. The accumulated FID signals were digitally filtered (50–100-Hz line broadening) to improve sensitivity. Spectral windows were 40 and 100 kHz at 15.09 and 62.98 MHz, respectively. Sample temperature was regulated within ±1 °C (Sarkar et al., 1983).

Spectra for measuring spin–lattice relaxation times (T_1) were obtained by using an inversion–recovery pulse sequence (180°–t–90°–T)$_n$. For each value of t, spectra were collected for the labeled sample as well as a control sample of the same weight. By subtracting the latter from the former, the integrated intensity for each value of t was corrected for natural abundance background. The integrated intensities were used in a least-squares analysis for T_1 determination. Nuclear Overhauser enhancements ($1 + \eta$) were measured as described by Sarkar et al. (1983). Because of signal to noise limitations at 15.09 MHz, natural abundance spectra were not subtracted from ^{13}C-labeled spectra when T_1 or NOE was measured. For this reason the uncertainty in these parameters is larger at the lower field as indicated in Table II.

THEORY

The primary goal of this paper is to obtain information about the dynamics of the collagen backbone from ^{13}C relaxation measurements. In particular, we want to determine the root mean square fluctuations in the azimuthal angle, γ_{rms}, of the collagen backbone. In order to do this we must develop equations that relate the measured NMR parameters (T_1 and NOE) to rotational correlation times and amplitudes.

X-ray diffraction data (Brodsky & Eikenberry, 1982) show that collagen molecules are most highly ordered in the direction parallel to the long axis of the molecule. We therefore assume that reorientation is primarily a consequence of motion about this axis (see Figure 1). This motion changes the orientation of the C^{α}–H bond axis, $\hat{\mu}$, relative to B_0 and therefore modulates the strong ^{13}C–^{1}H dipolar coupling producing spin–lattice relaxation. The dipolar coupling is the only significant relaxation mechanism since the chemical shift anisotropy of the α-carbon is small (≤50 ppm), and there is no quadrupole coupling since $I = {}^1/_2$. The general expressions for T_1 and NOE in the case of dipolar coupling are (Spiess, 1978)

$$1/T_1 = 1/T_1^{II} = (\omega_D^2/4)[J_0(\omega_I - \omega_S) + 3J_1(\omega_I) + 6J_2(\omega_I + \omega_S)] \quad (1)$$

$$NOE = 1 + \gamma_S T_1^{II}/(\gamma_I T_1^{IS}) \quad (2)$$

where

$$\omega_D = \hbar\gamma_I\gamma_S/r^3 \quad (3)$$

and

$$1/T_1^{IS} = (\omega_D^2/4)[-J_0(\omega_I - \omega_S) + 6J_2(\omega_I + \omega_S)] \quad (4)$$

The spectral density functions are defined as

$$J_m(\omega) = 2\int_0^{\infty} C_m(t) \cos(\omega t)\, dt \quad (5)$$

The correlation function, $C_m(t)$, is (Torchia & Szabo, 1982)

$$C_m(t) = \sum_{aa'=-2}^{2} d_{ma}^{(2)}(\theta) d_{ma'}^{(2)}(\theta) d_{0a}^{(2)}(\beta) d_{0a'}^{(2)}(\beta) \times \exp[i(a - a')\phi]\Gamma_{aa'}(t) \quad (6)$$

where (θ, ϕ) and (β, γ) are the respective polar angles that define the orientation of B_0 and $\hat{\mu}$ in the helix coordinate system (Figure 1) and

$$\Gamma_{aa'}(t) = \langle \exp[ia\gamma(0)] \exp[-ia'\gamma(t)] \rangle \quad (7)$$

We now evaluate $\Gamma_{aa'}$ explicitly for three models of motion.

(*1*) *Two-Site Jump Model.* Suppose $\hat{\mu}$ assumes two equally probable orientations, orientation 1 with (β, γ) = (β, $-\gamma_0$) and orientation 2 with (β, γ) = (β, $+\gamma_0$). By use of eq 23 in Torchia & Szabo (1982), the time-dependent part of $\Gamma_{aa'}(t)$ is given by

$$\Gamma_{aa'}(t) = \sin(a\gamma_{rms}) \sin(a'\gamma_{rms}) \exp(-\lambda t) \quad (8)$$

This formula is equivalent to eq 27 in Torchia & Szabo (1982) but differs in form because crystal-fixed coordinate systems are oriented differently in the two derivations of Γ. Note that $\gamma_0 = \gamma_{rms}$ for the two-site jump model.

(*2*) *Restricted Diffusion.* Suppose that $\hat{\mu}$ is restricted to free diffusion in the angular range $\pm\gamma_0$, then $\Gamma_{aa'}(t)$ is given by Wittebort & Szabo (1978).

(*3*) *Diffusion in a Harmonic Potential.* In this case it has been shown (Szabo, 1984) that the time-dependent part of $\Gamma_{aa'}$ is given by

$$\Gamma_{aa'}(t) = \exp[-\gamma_{rms}^2(a^2 + a'^2)/2] \sum_{n=1}^{\infty} (aa'\gamma_{rms}^2)^n \exp(-nDt/\gamma_{rms}^2)/n! \quad (9)$$

Previous studies of collagen backbone dynamics (Jelinski & Torchia, 1979; Jelinski et al., 1980; Sarkar et al., 1983) suggest that γ_{rms} is small. If $(a\gamma_{rms})^2 \ll 1$ rad, it is straightforward to show that

$$\Gamma_{aa'}(t) \simeq aa'\gamma_{rms}^2 \exp(-t/\tau) \quad (10)$$

for the two-site jump, restricted diffusion, and diffusion in harmonic potential models. Therefore, for each model the correlation function decays with a single correlation time and depends only upon γ_{rms}, not the details of the motion. The

fact that $\Gamma_{aa'}(t)$ depends only upon γ_{rms} for these distinctly different models of motion suggests that relaxation studies generally yield a model-independent value of γ_{rms} when $\gamma_{rms} \ll 1$ rad. It has been shown (Sarkar et al., 1983) that line shapes in the fast motion limit depend only on γ_{rms} when $\gamma_{rms} \ll 1$ rad.

Combining eq 1, 5, 6, and 10, we obtain

$$1/T_1 = [3\omega_D\gamma_{rms} \sin(\beta)/4]^2[\sin^4\theta[1 - \cos(4\phi)]g(\tau,\omega_I - \omega_S) + 2[\sin^2\theta + \sin^2(2\theta/4) + \sin^4\theta\cos(4\phi)]g(\tau,\omega_I) + [1 + 6\cos^2\theta + \cos^4\theta - \sin^4\theta\cos(4\phi)]g(\tau,\omega_I + \omega_S)] \quad (11)$$

where $g(\tau,\omega) = \tau/(1 + \omega^2\tau^2)$. In the fast limit $\omega^2\tau^2 \ll 1$, $g(\tau,\omega) \rightarrow \tau$ and

$$1/T_1 = (9\tau/4)(\omega_D\gamma_{rms} \sin\beta)^2(1 + \cos^2\theta) \quad (12)$$

Note that $1/T_1$ is independent of ϕ in the fast limit and varies by a factor of 2 as θ changes from 0° to 90°. The anisotropy (orientation dependence) of T_1 increases as τ increases. In the neighborhood of the T_1 minimum, $\omega\tau = 0.5$, there is a 4-fold variation in T_1 as orientation is varied.

We have not detected substantial T_1 anisotropy in the inversion–recovery spectra of the glycine α-carbon in collagen. We think that this is so because the anisotropy is averaged in several ways. To begin with, the glycine α-carbon is relaxed by two protons. Therefore, motions of two different internuclear vectors having different orientations relax the ^{13}C nucleus. Since the frequency of the ^{13}C signal is determined by the chemical shift interaction, the signal at each frequency will relax with two different rates determined by the different orientations of the two $\hat{\mu}$ vectors. Further averaging of T_1 anisotropy occurs because each frequency in the spectrum corresponds to a range of orientations of the C^α chemical shift tensor (Haeberlen, 1976). Therefore, each frequency component of the line shape relaxes with a range of T_1 values. The orientation- (frequency-) dependent relaxation of the signal cannot presently be calculated since the orientation of the glycine C^α shift tensor is not known. For this reason, and because the observed anisotropy in T_1 is small, we have measured and analyzed the relaxation function, $R(t)$, of the total signal intensity given by

$$R(t) = [M(t) - M_0]/[M(0) - M_0] \quad (13)$$

where $M(t)$ is the integrated signal intensity observed after the 180°–t–90° pulse sequence, $M(0)$ is $M(t)$ at $t = 0$, and M_0 is the equilibrium signal intensity. Since signal intensity corresponding to each orientation, (θ, ϕ), is a single exponential with time constant T_1 given by eq 11, $R(t)$ is a sum of exponentials given by

$$R(t) = [1/(4\pi)]\int \exp(-t/T_1)\, d\Omega \quad (14)$$

$$R(t) = [1/(4\pi)]\exp(-\bar{k}t)\int \exp[-(k - \bar{k})t]\, d\Omega \quad (15)$$

where $k = 1/T_1$, $\bar{k} = \langle k \rangle$, and $\langle\ \rangle$ designates integration over all Ω. Expanding the integrand in a Taylor series and integrating over $d\Omega$ leads to

$$R(t) = \exp(-\bar{k}t)(1 + k_{rms}^2t^2/2 + \ldots) \quad (16)$$

where

$$k_{rms}^2 = \langle k^2 \rangle - \langle k \rangle^2 \quad (17)$$

Because our inversion–recovery spectral data are obtained for small values of t, we find that plots of log $R(t)$ vs. t are linear for the collagen samples studied herein. Therefore, $k_{rms}^2t^2$ and higher order terms are evidently small enough to be ignored, and according to eq 16, the slope of the plot gives $\langle 1/T_1 \rangle$. The

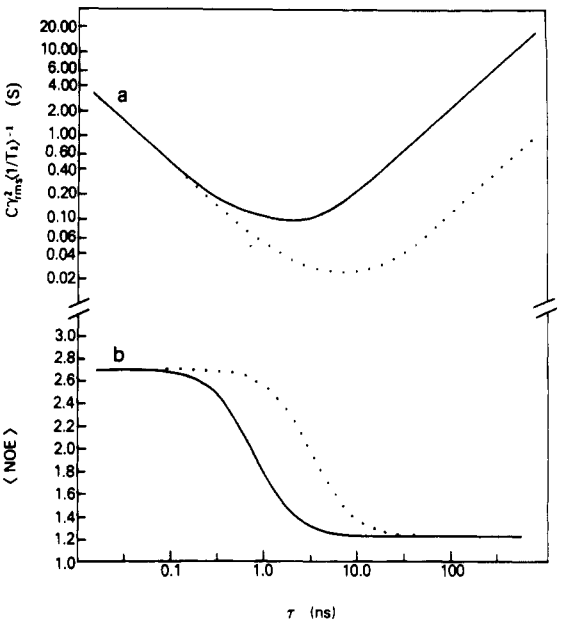

FIGURE 2: Averaged NMR parameters (a) $C\gamma_{rms}^2\langle 1/T_1\rangle^{-1}$ and (b) ⟨NOE⟩ calculated at two fields of 62.98 (—) and 15.09 MHz (···) assuming small amplitude fluctuations in the collagen azimuthal orientation (see eq 19 and 20).

explicit theoretical expression for $\langle 1/T_1 \rangle$, obtained by integrating eq 11 over $d\Omega$, is

$$\langle 1/T_1 \rangle = 3\gamma_{rms}^2(\sin^2\beta_1 + \sin^2\beta_2) \times (1/10)\omega_D^2[g(\tau,\omega_I - \omega_S) + 3g(\tau,\omega_I) + 6g(\tau,\omega_I + \omega_S)] \quad (18)$$

In this expression two terms involving the angle β appear because the Gly C^α is bonded to two protons. Using the atomic coordinates of the collagen model peptide $(Pro\text{-}Pro\text{-}Gly)_{10}$ (Okuyama et al., 1981), we calculate that $\sin^2\beta_1 + \sin^2\beta_2 = 1.76$. So eq 18 becomes

$$\langle 1/T_1 \rangle/(C\gamma_{rms}^2) = (1/10)\omega_D^2[g(\tau,\omega_I - \omega_S) + 3g(\tau,\omega_I) + 6g(\tau,\omega_I + \omega_S)] \quad (19)$$

where $C = 3(\sin^2\beta_1 + \sin^2\beta_2) = 5.28$. The expression on the left side of eq 19 is identical with that obtained for isotropic motion. Therefore, plots of $C\gamma_{rms}^2\langle 1/T_1 \rangle^{-1}$ vs. τ (Figure 2a) are the familiar curves obtained for isotropic motion in solution.

Although eq 19 was derived with the assumption that motion of $\hat{\mu}$ is restricted to reorientation about the helix axis, an essentially equivalent equation is obtained if $\hat{\mu}$ is assumed to wobble in a cone with semiangle $\beta \ll 1$ (Torchia & Szabo, 1982). The expression for $\langle 1/T_1 \rangle$ in this case is obtained simply by replacing $C\gamma_{rms}^2$ in eq 19 by $3[(\beta_1)_{rms}^2 + (\beta_2)_{rms}^2]$. So once again we see that for a small amplitude motion the essential information contained in the measurement of $\langle 1/T_1 \rangle$ is the rms amplitude of the angular fluctuation of $\hat{\mu}$.

The orientation averaged NOE is given by

$$\langle NOE \rangle = 1 + [(\gamma_S/\gamma_I)/(4\pi)]\int (T_1/T_1^{IS})\, d\Omega \quad (20)$$

Since $1/T_1$ and $1/T_1^{IS}$ are each proportional to γ_{rms}^2, ⟨NOE⟩ depends only upon τ. Plots of ⟨NOE⟩ vs. τ for the two field strengths used in this study are shown in Figure 2b. These curves in Figure 2b are similar to those obtained for isotropic motion; however, note that the limiting values of ⟨NOE⟩ are 2.7 and 1.23 in the fast ($\omega^2\tau^2 \ll 1$) and slow ($\omega^2\tau^2 \gg 1$) motion limits, respectively.

The procedure for obtaining γ_{rms} from the measured relaxation parameters is then as follows. We obtain τ from the measured value of ⟨NOE⟩ together with Figure 2b. Then we

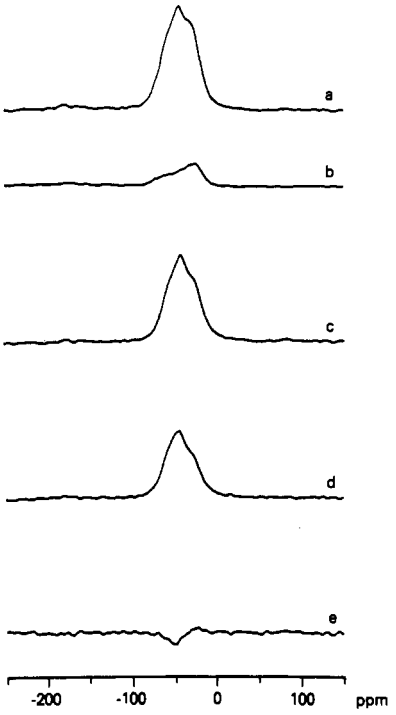

FIGURE 3: 62.98-MHz ^{13}C NMR spectra of rat tail tendon collagen (a) [2-^{13}C]glycine-labeled spectrum with NOE; (b) natural abundance spectrum with NOE; (c) difference spectrum obtained by subtracting spectrum b from spectrum a; (d) difference spectrum as obtained in (c) except that ^{13}C-labeled and natural abundance spectra were obtained without an NOE; (e) spectrum with zero integrated intensity obtained by subtracting 1.3 times spectrum d from spectrum c. All spectra were obtained at 22 °C by using a 90°–T pulse sequence, T = 2 s, and a 4.8-μs 90° pulse width. A total of 2048 transients was accumulated in each case, and the spectra shown have been normalized to compensate for different weights of labeled and natural abundance samples. Chemical shifts relative to external tetramethylsilane.

use this value of τ together with the curve in Figure 2a to determine $C\gamma_{rms}^2\langle 1/T_1\rangle^{-1}$. γ_{rms} is derived from the measured value of $\langle 1/T_1\rangle^{-1}$ and the definition of C (eq 19).

In the above discussion we have assumed that the potential functions that determine the rates and amplitudes of collagen backbone motions are time independent. Internal motion, as opposed to rigid body motion of a macromolecule like collagen, may involve a large number of degrees of freedom. If this is the case, local conformations in the neighborhood of $\hat{\mu}$ are time dependent. As a consequence the potential function may itself undergo large time-dependent fluctuations. When these fluctuations are rapid compared with $1/T_1$, reorientation of $\hat{\mu}$ is described by a (homogeneous) distribution of correlation times rather than a single correlation time even if $\gamma_{rms}^2 \ll 1$. We include the effect of a distribution of correlation times by replacing $\gamma_{rms}^2 g(\tau,\omega)$ in the expressions for $\langle 1/T_1\rangle$ and $\langle 1/T_1^{IS}\rangle$ by

$$\int \gamma_{rms}^2 g(\tau,\omega) p(\tau,\bar{\tau})\, d\tau$$

where $p(\tau,\bar{\tau})\, d\tau$ is the probability that the correlation time is in the range τ to $\tau + d\tau$, and $\bar{\tau}$ is the mean value of τ. William–Watts (Williams & Watts, 1970; Kaplan & Garroway, 1982) and log χ^2 distribution functions (Schaefer, 1973) have been used to analyze polymer relaxation data. Because NMR relaxation parameters are most sensitive to values of $\tau \sim \omega_I^{-1}$ we replace $\gamma_{rms}(\tau)$ by its average value in the neighborhood of ω_I^{-1}. For a log χ^2 distribution one then obtains plots of $\langle 1/T_1\rangle^{-1}$ and $\langle$NOE$\rangle$ vs. $\bar{\tau}$, similar to those given by Schaefer (1973) and Torchia et al. (1977). In this regard the major difference between the curves calculated for the single correlation and distribution of correlation time models is that the dependence of $\langle 1/T_1\rangle^{-1}$ and $\langle$NOE$\rangle$ on the correlation time and the field is much more gradual in the latter case.

Table I: Values of the Glycine α-Carbon Chemical Shift Tensor Principal Elements[a] in Collagen in Two Tissues at 22 and −35 °C

sample	σ_{xx} (ppm)	σ_{yy} (ppm)	σ_{zz} (ppm)
calvaria[b]	−24	−1	25
tail tendon[b]	−23	0	23
calvaria;[c] tail tendon[c]	−23	−4	27

[a] Tensor elements are relative to $\sigma_i = (\sigma_{xx} + \sigma_{yy} + \sigma_{zz})/3$ at 62.98 MHz; negative shifts indicate decreased shielding. [b] 22 °C; uncertainty ±3 ppm. [c] −35 °C; uncertainty ±3 ppm.

RESULTS

^{13}C spectra at 62.98 MHz of rat tail tendon collagen labeled with [2-^{13}C]glycine and in natural abundance are shown in Figure 3a,b, respectively. These spectra were obtained by using a 90°–T pulse sequence. The protons were decoupled during acquisition of the free induction decay signal and otherwise saturated to obtain an NOE. The difference spectrum, Figure 3c, obtained by subtracting the spectrum in Figure 3b from that in Figure 3a shows the [2-^{13}C]glycine powder pattern with an NOE. The difference spectrum in Figure 3d shows the [2-^{13}C]Gly powder pattern without NOE. As expected, the signal in Figure 3c is larger than that in Figure 3d. In addition, the signal shapes differ slightly because the NOE is anisotropic. This is seen in the difference spectrum, Figure 3e, obtained by multiplying the signal in Figure 3d by the average NOE and subtracting this signal from the signal in Figure 3c. Although the resulting spectrum has no net signal, it is composed of small positive and negative components because the NOE is anisotropic.

Since the spectrum in Figure 3d is corrected for natural abundance contributions and has no NOE, we have obtained the principal elements of the [2-^{13}C]Gly chemical shift tensor by computer simulating this line shape. The principal elements obtained by this procedure are listed in Table I for collagen in the various samples at 22 and −35 °C. The experimental uncertainties in the tensor elements are large because line widths of nearly 10 ppm had to be employed in order to obtain good simulations of the observed spectra. These large line widths are a consequence of (a) the short $T_{1\rho}$ of the glycine α-carbons, $\lesssim$1 ms, (b) chemical shift dispersion of 2–3 ppm, resulting from variations in sequence and structure, and (c) the 100-Hz line broadening used to improve signal to noise. As shown previously (Sarkar et al., 1983) ^{13}C–^{14}N dipolar coupling is not large ($\lesssim$3 ppm) in collagen at 62.98 MHz at the temperatures used because the ^{14}N T_1 is small enough to decouple these nuclei.

Spin–lattice relaxation times were obtained from inversion–recovery difference spectra like those shown in Figure 4 for rat tail tendon. The relaxation is slightly anisotropic, like the NOE, and different parts of the powder pattern relax with different rates. Because the anisotropy in T_1 has a small effect on the partially relaxed line shape and because the orientation of the glycine α-carbon chemical shift tensor is not known, we used the integrated intensity of the entire signal to determine the average T_1 value. The average T_1 values obtained for the various samples at 15.09 and 62.98 MHz and at 22 and −35 °C are listed in Table II. The average NOE values measured at the two fields and temperatures are also listed in Table II.

The correlation times for the six collagen samples (Table III) are obtained at 22 °C and 62.98 MHz from the plot of

Table II: Measured Values[a] of $\langle 1/T_1 \rangle^{-1}$ and $\langle$NOE$\rangle$ for Glycine α-Carbons in Collagen Samples at Two Fields and Temperatures

	62.98 MHz at					
	22 °C		−35 °C		15.09 MHz at 22 °C	
sample	$\langle 1/T_1 \rangle^{-1}$ (s)	$\langle$NOE$\rangle$	$\langle 1/T_1 \rangle^{-1}$ (s)	$\langle$NOE$\rangle$	$\langle 1/T_1 \rangle^{-1}$ (s)	$\langle$NOE$\rangle$
reconstituted fibrils	0.7	1.4	7.5	2.0	0.13[b]	1.7[b]
tail tendon	0.8	1.3	8.3	1.4	0.24	1.6
demineralized calvaria	0.8	1.6				
demineralized tibia	0.8	1.6				
mineralized calvaria	1.9	1.6	7.9	1.6	0.54	1.6
mineralized tibia	1.8	1.4	8.2	1.4	0.63	1.6

[a] Experimental uncertainty: 10% at 62.98 MHz and 20% at 15.09 MHz. [b] From Jelinski & Torchia (1979).

Table III: Values of τ and γ_{rms} Obtained for Collagen Samples at 22 °C from Glycine α-Carbon $\langle$NOE$\rangle$ and $\langle 1/T_1 \rangle^{-1}$ Measurements

	62.98 MHz		15.09 MHz	
sample	τ (ns)	γ_{rms} (deg)	τ (ns)	γ_{rms} (deg)
reconstituted fibrils	2.0	9.4	4.8	10.8
tail tendon	3.2	9.4	5.6	8.0
demineralized calvaria	1.2	8.8		
demineralized tibia	1.2	8.8		
mineralized calvaria	1.2	5.8	5.6	5.3
mineralized tibia	2.0	5.9	5.6	4.9

$\langle$NOE$\rangle$ vs. τ (Figure 2b) together with the measured $\langle$NOE$\rangle$ values. These correlation times and Figure 2a yield theoretical values of $C\gamma_{rms}^2 \langle 1/T_1 \rangle^{-1}$. Since C is known, the measured values of $\langle 1/T_1 \rangle^{-1}$ yield the values of γ_{rms} (Table III). Values of τ and γ_{rms} (Table III) were obtained in a similar way at −35 °C and 62.98 MHz and at 22 °C and 15.09 MHz.

Discussion

The correlation times obtained for the various collagen samples at 22 °C, 62.98 MHz, lie in the range 1–3 ns. At the same temperature, but at the lower field strength, 15.09 MHz, correlation times for all samples are larger, 5–6 ns. This discrepancy in correlation times derived at the two different field strengths is explained by the fact that the theoretical curves in Figure 2b, which are calculated assuming small amplitude fluctuations in the collagen azimuthal angle, predict a large difference in $\langle$NOE$\rangle$ values at the two field strengths when τ is in the range 0.5–5 ns. In fact, the measured values of $\langle$NOE$\rangle$ (Table II) are only slightly larger at 15.09 MHz than at 62.98 MHz.

If we relax our assumption that γ_{rms} is small and allow γ_{rms} to have large values, major discrepancies between theory and experiment are found. Analysis of the T_1 data shows that when γ_{rms} is greater than 20°, $(\omega_1\bar{\tau})^2$ is either much greater or much less than one. [$\bar{\tau}$ is the mean correlation time and is equal to the derivative of $\Gamma_{aa}(t)$ at $t = 0$]. For values of $(\omega_1\bar{\tau})^2$ in these limits, the predicted (a) field dependence of T_1 and (b) values of $\langle$NOE$\rangle$ are either much greater than or much less than that observed.

In contrast with these results, theory does predict the observed small field dependence of $\langle$NOE$\rangle$ if a log χ^2 distribution ($p = 14$, $b = 1000$) is used (Schaefer, 1973; Torchia et al., 1977), and the values of γ_{rms} obtained are 20–30% larger than those listed in Table III. A simple two-component correlation function

$$C_m(t) = (6/10) \sin^2 \beta[(\gamma_A)_{rms}^2 \exp(-t/\tau_A) + (\gamma_B)_{rms}^2 \times \exp(-t/\tau_B)] \quad (21)$$

also predicts a small field dependence of $\langle$NOE$\rangle$ and yields a consistent analysis of the relaxation data. For example, the measured relaxation parameters of the tendon sample are calculated by using $\tau_A = 1.5$ ns, $(\gamma_A)_{rms} = 10°$, $\tau_B = 50$ ns, and $(\gamma_B)_{rms} = 20°$. Again the value of γ_{rms} for the fast motion component is slightly larger than the result in Table III. We have not pursued calculations using multicomponent correlation functions in great detail for two reasons. First, our preliminary calculations indicate that the values of γ_{rms} obtained do not differ greatly from the single correlation time results in Table III. Second, multicomponent correlation functions contain additional unknown parameters which can be constrained only when many more field-dependent measurements are made. When such measurements are made, it will be valuable to consider multicomponent correlation functions in detail since they model the complex motion of the collagen backbone better than the simple model used herein.

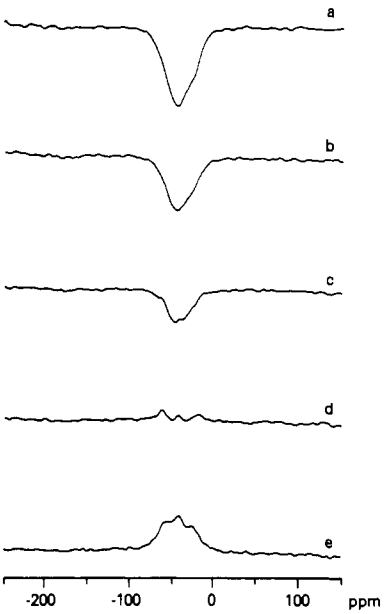

FIGURE 4: 62.98-MHz ^{13}C NMR inversion–recovery spectra of rat tail tendon collagen at 22 °C obtained by using a 180°–t–90°–T pulse sequence with $T = 2$ s and t = (a) 0.1, (b) 0.2, (c) 0.3, (d) 0.5, and (e) 0.75 s. Each spectrum is the difference of the inversion–recovery spectrum of [2-^{13}C]glycine-labeled collagen and the corresponding inversion–recovery spectrum of collagen in natural abundance. Chemical shifts relative to external tetramethylsilane.

Examination of Table III shows that, for a given sample, the values of γ_{rms} obtained at the two field strengths are in close agreement. If we average the values of γ_{rms} obtained for the various types of samples at the two fields, we find that $\gamma_{rms} = 5.5°$ for the mineralized cross-linked bone collagen samples, $\gamma_{rms} = 8.8°$ for the nonmineralized cross-linked samples, and $\gamma_{rms} = 10.1°$ for the nonmineralized non-cross-linked reconstituted sample.

Before the significance of these results is discussed, it is necessary to comment upon their accuracy. Several sources of error contribute to the uncertainty in the values of γ_{rms} listed in Table III. To begin with, the measured values of $\langle$NOE$\rangle$

and Figure 2b show that τ is approximately equal to ω_I^{-1}, but the value of τ is quite sensitive to errors in the ⟨NOE⟩ measurement which causes the values of τ listed in Table III to have an uncertainty of nearly a factor of 2. Fortunately, the large uncertainty in τ translates into a much smaller uncertainty, nearly 20%, in $C\gamma_{rms}^2\langle 1/T_1\rangle^{-1}$ because, according to Figure 2a, this quantity is insensitive to τ when $\tau \sim \omega_I^{-1}$. Other errors in γ_{rms}, nearly 30%, arise from the combined uncertainties in C, $\langle 1/T_1\rangle$, and ω_D. It should also be recalled that distribution of correlation time models suggest that the single correlation time model underestimates γ_{rms} by 20–30%. As a consequence of these sources of error the values of γ_{rms} listed in Table III are accurate only to within a factor of 1.5. However, it is important to realize that, except for the error in measuring $\langle 1/T_1\rangle^{-1}$, all other sources of error affect γ_{rms} for each sample in the same way. Therefore, the ratios of the values of γ_{rms} have uncertainties of less than 10%, and the progressive reduction of γ_{rms} seen in Table III provides a quantitative estimate of the extent to which cross-linking and mineralization restrict nanosecond motions of the collagen backbone. A qualitatively similar progression in γ_{rms} values was found (Sarkar et al., 1983) from an analysis of the line shapes of collagens labeled with [1-^{13}C]glycine; however, the values of γ_{rms} obtained from the line-shape analyses were 3–4 times larger than the values obtained herein. Although we have noted that the absolute values of γ_{rms} have large uncertainties, we do not think that this explains the large differences in γ_{rms} observed in the two types of experiments. Rather, we think the difference in values of γ_{rms} is found because T_1 and NOE values are primarily sensitive to motions having correlation times of ca. 1 ns; in contrast, all motions having correlation times less than ca. 10^{-4} s will affect the [1-^{13}C]glycine line shape. Therefore, slow motions having large amplitudes will be sensed by the line shape but not the relaxation times.

At −35 °C and 62.98 MHz the measured values of $\langle 1/T_1\rangle^{-1}$ are 5–10 times larger than the values measured at 22 °C, whereas the measured ⟨NOE⟩ values are the same, within experimental error, at the two temperatures. These measurements imply that the collagen correlation times are in the 1–3-ns range at −35 °C as found at 22 °C. However, in contrast with the results obtained at 22 °C, a small value of γ_{rms}, 3°, is obtained for all collagen samples (mineralized and nonmineralized) at −35 °C. This value of γ_{rms} may be an overestimate since the measured values of $\langle 1/T_1\rangle^{-1}$ are so large at −35 °C (Table II) that the ^{13}C–^{13}C spin diffusion may affect the measurement of $\langle 1/T_1\rangle^{-1}$. For instance, rapidly relaxing methyl carbons may contribute to the relaxation of the glycine α-carbons.

The low-temperature relaxation results are in accord with studies of [1-^{13}C]glycine line shapes in collagen at −35 °C where rigid lattice powder line shapes are observed without distortion from ^{13}C–^{14}N dipolar coupling. A line-shape calculation shows that a motion having γ_{rms} = 3° produces an insignificant reduction (<1%) in the rigid lattice chemical shift powder line width of the glycine carbonyl carbon; at the same time, modulation of the strong nitrogen quadrupole interaction by this motion results in rapid spin–lattice relaxation of the peptide nitrogen, thereby reducing the ^{14}N–^{13}C dipolar coupling.

The NMR studies of collagen backbone dynamics show that the amplitude of backbone motion is not greatly affected by cross-links. This result is reasonable since collagen fibers contain only a few intermolecular cross-links per molecule (Eyre, 1980). These studies also provide insight into the nature of the backbone motions. Motions having correlation times in the range of a few nanoseconds have been observed. Since these correlation times are much smaller than the correlation times calculated for overall motion of the molecule (Jelinski & Torchia, 1979), the backbone motion must be segmental. Motion of a long segment wil have a larger correlation time and amplitude than motion of a short segment. This is in accord with the result that γ_{rms} obtained from line-shape analysis ($\tau < 10^{-4}$ s) is 3–4 times larger than γ_{rms} obtained from relaxation data ($\tau \sim$ 1–3 ns). The observation that all samples studied have small values of γ_{rms} ($\sim$3°) when bulk water is frozen (−35 °C) suggests that mobile (liquidlike) water has an important role in collagen flexibility. This conclusion is supported by the observation that γ_{rms} is much smaller in intact bone and lyophilized demineralized bone samples than in hydrated nonmineralized samples. In bone, most of the water has been replaced by a rigid inorganic matrix (calcium phosphate) (Eanes et al., 1976). Presumably the interaction of mineral with collagen hinders motion of the collagen molecules. However, since collagen backbone motion involves segments of unknown length, we cannot estimate the frequency of collagen–mineral interactions along the surface of the triple helix using the present data. Amino acid side chains are located on the surface of the collagen molecules (Bornstein & Traub, 1979) and are flexible in unmineralized collagen fibrils (Torchia, 1984). We are currently comparing the flexibility of various labeled amino acid side chains in mineralized and nonmineralized collagen to characterize collagen–mineral interactions in greater detail.

We conclude with a discussion of the possible functional significance of collagen backbone mobility. Collagen fibers provide mechanical stability in connective tissues by virtue of their high tensile strength. One possible benefit of molecular flexibility is that collagen molecules are able to make rapid, small conformational changes as tension is applied, which permits stress to be distributed uniformly. In addition, some of the mechanical energy associated with the application of tension can be absorbed by the segmentally flexible molecules. The conformational freedom of demineralized collagen molecules suggests that the unmineralized collagen matrix is able to accommodate calcium phosphate crystallites having a variety of shapes and sizes. Although mineralization reduces collagen flexibility, the remaining molecular motions may contribute to the impact strength of bone just as molecular motion is thought (Steger et al., 1980) to contribute to impact strength of solid polymers.

ACKNOWLEDGMENTS

We have benefited from helpful discussions with Dr. Attila Szabo on the theoretical aspects of this paper, and we thank N. Whittaker for the mass spectrometry.

REFERENCES

Bornstein, P., & Traub, W. (1979) *Proteins (3rd Ed.) 4*, 411–632.

Brodsky, B., & Eikenberry, E. F. (1982) *Methods Enzymol. 82*, 127–174.

Caravatti, P., Deli, J. A., Bodenhausen, G., & Ernst, R. R. (1982) *J. Am. Chem. Soc. 104*, 5506–5507.

Eanes, E. D. (1973) in *Biological Mineralization* (Zipkin, I., Ed.) pp 227–256, Wiley, New York.

Eanes, E. D., Martin, G. N., & Lundy, D. R. (1976) *Calcif. Tissue Res. 20*, 313–316.

Eyre, D. R. (1980) *Science (Washington, D.C.) 207*, 1315–1322.

Haeberlen, U. (1976) *Adv. Magn. Reson., Suppl. 1*, 1–190.
Henrichs, P. M., & Linder, M. (1984) *J. Magn. Reson. 58*, 458–461.
Jelinski, L. W., & Torchia, D. A. (1979) *J. Mol. Biol. 133*, 45–65.
Jelinski, L. W., Sullivan, C. E., Batchelder, L. S., & Torchia, D. A. (1980) *Biophys. J. 32*, 515–529.
Kaplan, J. I., & Garroway, A. N. (1982) *J. Magn. Reson. 49*, 464–475.
Okuyama, K., Okuyama, K., Arnott, S., Takayanagi, M., & Kakudo, M. (1981) *J. Mol. Biol. 152*, 427–443.
Sarkar, S. K., Sullivan, C. E., & Torchia, D. A. (1983) *J. Biol. Chem. 258*, 9762–9767.
Schaefer, J. (1973) *Macromolecules 6*, 882–888.
Speiss, H. W. (1978) *NMR: Basic Princ. Prog. 15*, 55–214.
Steger, T. R., Schaefer, J., Stejskal, E. O., & McKay, R. A. (1980) *Macromolecules 13*, 1127–1132.
Szabo, A. (1984) *J. Chem. Phys. 81*, 150–167.
Szeverenyi, N. M., Sullivan, M. H., & Maciel, G. E. (1982) *J. Magn. Reson. 47*, 462–475.
Torchia, D. A. (1984) *Annu. Rev. Biophys. Bioeng. 13*, 125–144.
Torchia, D. A., & Szabo, A. (1982) *J. Magn. Reson. 49*, 107–121.
Torchia, D. A., Hasson, M. A., & Hascall, V. C. (1977) *J. Biol. Chem. 252*, 3617–3625.
Williams, G., & Watts, D. C. (1970) *Trans. Faraday Soc. 66*, 85–88.
Wittebort, R. J., & Szabo, A. (1978) *J. Chem. Phys. 69*, 1722–1736.

Aminoacylation of Anticodon Loop Substituted Yeast Tyrosine Transfer RNA†

Lance Bare and Olke C. Uhlenbeck*
Department of Biochemistry, University of Illinois, Urbana, Illinois 61801
Received July 3, 1984; Revised Manuscript Received November 9, 1984

ABSTRACT: A procedure for replacing residues 33–35 in the anticodon loop of yeast $tRNA^{Tyr}$ with any desired oligonucleotide has been developed. The three residues were removed by partial ribonuclease A digestion. An oligonucleotide was inserted into the gap in four steps by using RNA ligase, polynucleotide kinase, and *pseT* 1 polynucleotide kinase. The rate of aminoacylation of anticodon loop substituted $tRNA^{Tyr}$ by yeast tyrosyl-tRNA synthetase was found to depend upon the sequence of the oligonucleotide inserted. This suggests that the nucleotides in the anticodon loop of yeast $tRNA^{Tyr}$ are required for optimal aminoacylation. In addition, $tRNA^{Tyr}$ modified to have a phenylalanine anticodon was shown to be misacylated by yeast phenylalanyl-tRNA synthetase at a rate at least 10 times faster than unmodified $tRNA^{Tyr}$. Thus, the anticodon is used by phenylalanyl-tRNA synthetase to distinguish between tRNAs.

When a tRNA reacts with its cognate aminoacyl-tRNA synthetase, the anticodon loop is often in contact with the surface of the enzyme. Kisselev (1983) summarizes a variety of experiments indicating the involvement of the anticodon for eight different *Escherichia coli* and five different yeast tRNA synthetases. In several instances, it is clear that functional groups of anticodon nucleotides are important in the interaction. If anticodon residues 34 or 35 of *E. coli* $tRNA_f^{Met}$ are chemically modified (Schulman & Pelka, 1977) or altered in their sequence (Schulman et al., 1983a), the rate of aminoacylation is drastically reduced. Mutations in the anticodons of *E. coli* $tRNA^{Gly}$ (Carbon & Squires, 1971) and $tRNA^{Trp}$ (Yarus et al., 1977) also have been shown to alter their rate of aminoacylation. These experiments support the view that anticodon loop residues could be used by aminoacyl-tRNA synthetases to distinguish between different tRNAs (Kisselev & Frolova, 1964).

In this work, we describe an enzymatic procedure to alter the sequence of residues 33–35 of yeast $tRNA^{Tyr}$ to any desired sequence. The procedure closely resembles the protocol previously developed for substituting nucleotides 34–37 in yeast $tRNA^{Phe}$ (Bruce & Uhlenbeck, 1982a) although different anticodon residues are changed. We have used these anticodon-substituted $tRNAs^{Tyr}$ to demonstrate that yeast tyrosyl-tRNA synthetase also requires the correct anticodon sequence for optimal rates of aminoacylation. In addition the substitution of Ψ-35 with an A produces a $tRNA^{Tyr}$ with a phenylalanine anticodon. Since it has been shown previously that yeast phenylalanyl-tRNA synthetase requires the correct anticodon sequence in $tRNA^{Phe}$ to give an optimal rate of aminoacylation (Bruce & Uhlenbeck, 1982b), the misacylation of the A-35 $tRNA^{Tyr}$ with phenylalanyl-tRNA synthetase was investigated. We show that the substitution results in a substantial increase in misacylation when compared to $tRNA^{Tyr}$. These results clearly indicate that a contact at A-35 is important in the interaction of the tRNA with phenylalanyl-tRNA synthetase.

Materials and Methods

Enzymes. RNA ligase (Moseman-McCoy et al., 1979) and polynucleotide kinase (Cameron & Uhlenbeck, 1977) were purified from T4-infected *E. coli*. Polynucleotide kinase lacking the 3′-phosphatase activity was purified from *pseT* 1 T4 infected *E. coli* (Soltis & Uhlenbeck, 1982). Primer-dependent polynucleotide phosphorylase was purified from *Micrococcus luteus* (Klee, 1971). Yeast tRNA nucleotidyltransferase was a gift from P. Sigler. Homogeneous yeast phenylalanyl-tRNA synthetase was a gift from P. Remy. Yeast tyrosyl-tRNA synthetase was purified to a specific activity of 200 units/mg by using the first three steps of the procedure of Faulhammer & Cramer (1977). Ribonucleases T_1, T_2, P_1, and Cl_3 were purchased from Boehringer-Mann-

† This work was supported by a grant from the National Institutes of Health (GM 30418).

0006-2960/85/0424-2354$01.50/0